

X-RAY STATES OF REDBACK MILLISECOND PULSARS

M. LINARES^{1,2}

Accepted for publication in The Astrophysical Journal

ABSTRACT

Compact binary millisecond pulsars with main-sequence donors, often referred to as “redbacks”, constitute the long-sought link between low-mass X-ray binaries and millisecond radio pulsars, and offer a unique probe of the interaction between pulsar winds and accretion flows. We present a systematic study of eight nearby redbacks, using more than 100 observations obtained with *Swift*’s X-ray Telescope. We distinguish between three main states: pulsar, disk and outburst states. We find X-ray mode switching in the disk state of PSR J1023+0038 and XSS J12270–4859, similar to what was found in the other redback which showed evidence for accretion: rapid, recurrent changes in X-ray luminosity (0.5–10 keV, L_X), between $[6-9] \times 10^{32}$ erg s^{−1} (disk-passive state) and $[3-5] \times 10^{33}$ erg s^{−1} (disk-active state). This strongly suggests that mode switching—which has not been observed in quiescent low-mass X-ray binaries—is universal among redback millisecond pulsars in the disk state. We briefly explore the implications for accretion disk truncation, and find that the inferred magnetospheric radius in the disk state of PSR J1023+0038 and XSS J12270–4859 lies outside the light cylinder. Finally, we note that all three redbacks which have developed accretion disks have relatively high L_X in the pulsar state ($>10^{32}$ erg s^{−1}).

Subject headings: accretion, accretion disks — pulsars: individual(PSR J1023+0038, XSS J12270–4859, PSR J1628–32, PSR J1723–28, PSR J1816+4510, PSR J2129–0429, PSR J2215+5135, PSR J2339–0533)— stars: neutron — X-rays: binaries — X-rays: individual (PSR J1023+0038, XSS J12270–4859, PSR J1628–32, PSR J1723–28, PSR J1816+4510, PSR J2129–0429, PSR J2215+5135, PSR J2339–0533)

1. INTRODUCTION

During the last five years, the connection between rotation-powered millisecond radio pulsars (MRPs) and accretion-powered low-mass X-ray binaries (LMXBs) has been firmly established on an observational basis. Conclusive evidence for accretion has been found in three systems that have also been directly detected as rotation-powered MRPs: PSR J1023+0038 (J1023 hereafter; Archibald et al. 2009), PSR J1824–2452/IGR J18245–2452 (M28-I hereafter, in the globular cluster M28; Papitto et al. 2013) and XSS J12270–4859 (J12270 hereafter; de Martino et al. 2010, 2013a; Roy, Bhattacharyya & Ray 2014). This is the strongest confirmation of the so-called “recycling scenario” for MRP formation, where neutron stars are spun up by the accretion of matter in an LMXB phase (Alpar et al. 1982). It has also become clear (Papitto et al. 2013; Stappers et al. 2014) that the evolution from the LMXB to the MRP phase does not involve a sharp “accretion turn-off”, and multiple MRP↔LMXB transitions can actually take place (as predicted by some evolutionary models, Tauris 2012).

In all three LMXB-MRP transition pulsars (J1023, M28-I and J12270) the neutron star is in a close orbit (period $P_{\text{orb}} \simeq 4-11$ hr) with a low-mass main-sequence companion star (with mass $M_C \gtrsim 0.1-0.5 M_\odot$). From the radio pulsar point of view, this classifies all three transition pulsars as “redbacks” (Roberts 2013), a name inspired by the strong irradiation of the companion in anal-

ogy with the “black widow” pulsars (which have ~ 10 times lower M_C ; Fruchter, Stinebring & Taylor 1988). All three transition pulsars are redbacks, but not all known redbacks have been observed in an accretion state. It is therefore natural to study in depth all redback MRPs to understand how the LMXB-MRP transition occurs and to search for more transition systems.

Non-thermal X-ray emission modulated at the orbital period has been observed in both black widow (Stappers et al. 2003) and redback MRPs (in the “pulsar state”, see Secs. 3 & 6 for definition; Bogdanov, Grindlay & van den Berg 2005; Bogdanov et al. 2011a, 2014b), with X-ray luminosities (L_X , 0.5–10 keV) of $\sim 10^{31}-10^{32}$ erg s^{−1}. This is typically ascribed to Doppler-boosted and partially occulted intra-binary shock emission (Arons & Tavani 1993). Thermal pulsed X-rays from the heated polar caps are also detected from some MRPs, with typical $L_X \sim 10^{30}$ erg s^{−1}. Similarly, the quiescent X-ray spectrum of neutron star LMXBs can be broadly divided into a thermal component powered by incandescent crustal emission or residual surface accretion (Brown, Bildsten & Rutledge 1998; Wijnands et al. 2001), and a non-thermal component of less certain origin (Campana et al. 1998a).

Using *Chandra* observations of M28-I in quiescence, Linares et al. (2014a) discovered X-ray mode switching: rapid transitions between active ($L_X \sim 10^{33}$ erg s^{−1}) and passive ($L_X \sim 10^{32}$ erg s^{−1}) states. They interpreted these as fast transitions between magnetospheric accretion and pulsar wind shock emission as the neutron star magnetospheric radius moves in and out of the light cylinder (see Linares et al. 2014a, for details; see also Ferrigno et al. 2014, for peculiar variability at higher L_X). Besides

¹ Instituto de Astrofísica de Canarias, c/ Vía Láctea s/n, E-38205 La Laguna, Tenerife, Spain

² Universidad de La Laguna, Departamento de Astrofísica, E-38206 La Laguna, Tenerife, Spain

M28-I (Begin 2006), a number of redbacks have been found in globular clusters (GCs) (Camilo et al. 2000; D’Amico et al. 2001; Possenti et al. 2003). Even if they may also occasionally undergo accretion episodes, multi-wavelength monitoring of MRPs in GCs is challenging due to a combination of large distance, strong absorption, crowded fields and acceleration within the cluster.

Thanks to the numerous GeV sources discovered with *Fermi*’s Large Area Telescope (LAT, Abdo et al. 2010; Nolan et al. 2012), a new population of nearby redback MRPs in the Galactic plane has been uncovered (Hessels et al. 2011; Ray et al. 2012; Roberts 2013). Like J1023 and J12270, these recently discovered redbacks have the advantage of being nearby (distance $D \lesssim 4$ kpc), barely absorbed (equivalent hydrogen column densities $N_H \lesssim 10^{21} \text{ cm}^{-2}$) and in non-crowded fields. This makes them accessible to a broader range of space and ground-based observatories, allowing much more frequent monitoring.

In this work we assemble the current sample of nearby redbacks in the Galactic field, a total of eight systems including J1023 and J12270, and study their properties using all available observations taken with the X-ray telescope (XRT) aboard the *Swift* observatory. We define three main states of redback MRPs: pulsar, disk and outburst state³. We find X-ray mode switching in the disk state of J1023 and J12270 (Patruno et al. 2014; de Martino et al. 2013a), in clear analogy with M28-I (Linares et al. 2014a). We also study the luminosity of the pulsar state using the full sample of redbacks, report two candidates for the X-ray counterpart of PSR J2129–0429 and suggest two promising targets to search for future transitions to the disk state: PSR J1723–2837 and PSR J2215+5135. Our main results and conclusions are summarized in Section 6.

2. ANALYSIS

We analyzed all *Swift*-XRT observations of the following eight redbacks available in March 2014: J1023, J12270, PSR J1628–32 (J1628 hereafter), PSR J1723–28 (J1723), PSR J1816+4510 (J1816), PSR J2129–0429 (J2129), PSR J2215+5135 (J2215) and PSR J2339–0533 (J2339; see details and references for each source in Table 1 & Section 3). This yielded 107 observations with a total on-source exposure time of 190 ksec. All observations were taken in imaging mode (photon counting, PC) except for nine short non-imaging pointings that were not included in this analysis (windowed timing, totalling less than 0.9 ksec). Table 1 shows a summary of the resulting source sample and dataset as well as the values of D and N_H used in this work.

All data and auxiliary products were created using generic (v. 6.12) and *Swift*-specific (v. 3.9.28) FTOOLS with the latest CALDB calibration files, after creating reprocessed event files using XRTPIPELINE (v. 0.12.6). In the case of J2129 (Sec. 3.5), as no accurate (arcsecond) location has been reported, we calculated positions for our two counterpart candidates using *Swift* UKSSDC’s

online tool⁴, with both the point-spread function (PSF) and the UVOT-enhanced methods (Goad et al. 2007; Evans et al. 2009, which corrects the absolute astrometry using nearby UV sources with accurate locations). We also verified that the positions given by XRTCENTROID (v. 0.2.9) are consistent with the UVOT-enhanced locations reported below.

We extracted source and background spectra within XSELECT (v. 4.2b) using circular regions with 20–30” and 60” radius, respectively. We created ancillary response files using exposure maps (combining multiple observations within XIMAGE, v. 4.5.1, when necessary), thereby taking into account dead pixels/columns and XRT’s PSF. Using the latest response matrices (v. 014) from the CALDB database, we fitted all 0.5–10 keV source spectra within XSPEC (v. 12.7.1, Arnaud 1996) grouping the spectra to a minimum of 10 counts per spectral bin, or using Cash’s C-statistic for spectra with low number of source counts ($\lesssim 50$).

Errors on spectral parameters are given at the 68% confidence level (c.l.). When N_H was unconstrained in the XRT spectral fits, we fixed it to literature values if available, or to the total Galactic value in the line of sight (Kalberla et al. 2005, see Table 1). For the two sources not detected, we calculated 90% c.l. L_X upper limits using a 30” region, the D and N_H values given in Table 1 and assuming a power law spectrum with photon index Γ in the 1–2 range. In only three cases (J1628, J2129 and J2215) we use D measurements that rely exclusively on the pulsar’s dispersion measure (Ray et al. 2012, which at high Galactic latitudes may underestimate D by a factor 2, Roberts 2011). The distance to J12270 is only constrained between 1.4 and 3.6 kpc (de Martino et al. 2013a). For this particular source we use the full 1.4–3.6 kpc range when quoting L_X uncertainties, although we favor the shortest D value as explained in Section 3.1. In all other sources we use the statistical uncertainty on the flux measurements when quoting L_X uncertainties.

We also extracted barycentered light curves in the full (0.3–10 keV) XRT energy band from the two brightest sources, J1023 and J12270, using time bins in the 150–300 s range and a 30” radius extraction region. Dead pixels and columns combined with different pointings can introduce XRT count rate variations that are not intrinsic to the source. We verified that such exposure correction (which we apply to the energy spectra as explained above) does not change the count rate distribution in the light curves significantly. To do so, we corrected each orbit’s light curve separately applying correction factors derived from the corresponding exposure maps (using XRTLCCORR and LCMATH)⁵. This correction typically increases the count rate by 20–30% (about 10 times more in a few orbits with bad geometry, where several dead columns cross the source extraction region). We find that the count rate distributions obtained from the exposure-corrected and original/uncorrected light curves are fully consistent, and we use the latter hereafter. The light curves are not background subtracted; we measure an average background rate using a 30” region of 7×10^{-4} and 5×10^{-4} c/s in J1023 and J12270, respectively, i.e. more than ten times lower than the collected source count

³ Note that the presence of an accretion disk in the disk state has been established by the detection of broad double-peaked optical emission lines, even if an accretion disk component has not been detected to date in its X-ray spectrum. See, e.g., Archibald et al. (2009) and Sections 3.1 & 4.

⁴ http://www.swift.ac.uk/user_objects/

⁵ <http://www.swift.ac.uk/analysis/xrt/lccorr.php>

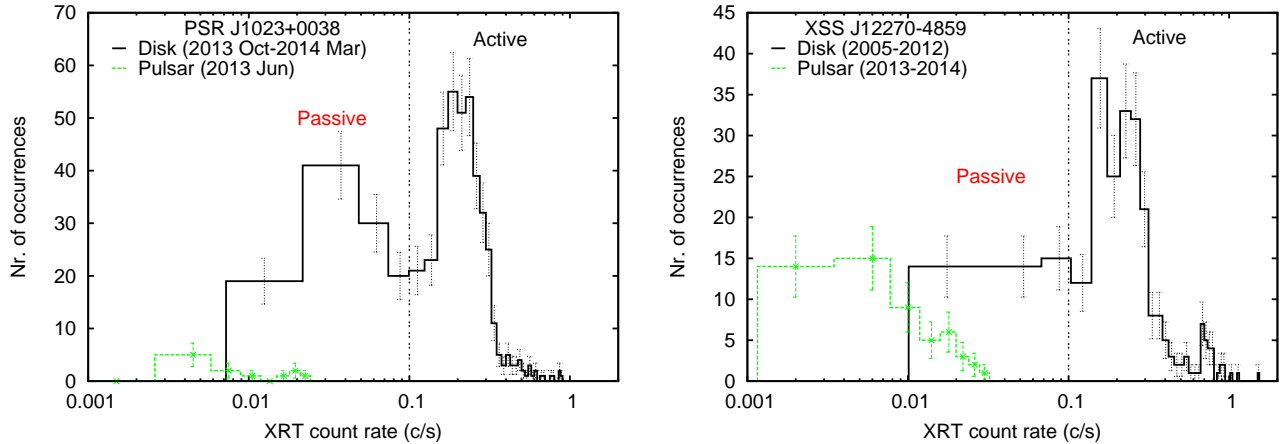


FIG. 1.— Count rate distribution in the 0.3–10 keV XRT light curves of J1023 (*left*) and J12270 (*right*). The disk state (solid black histogram) and pulsar state (dashed green histogram) are shown separately. The horizontal dotted line at 0.1 c s⁻¹ marks the boundary between disk-active and disk-passive states (labeled in black and red, respectively).

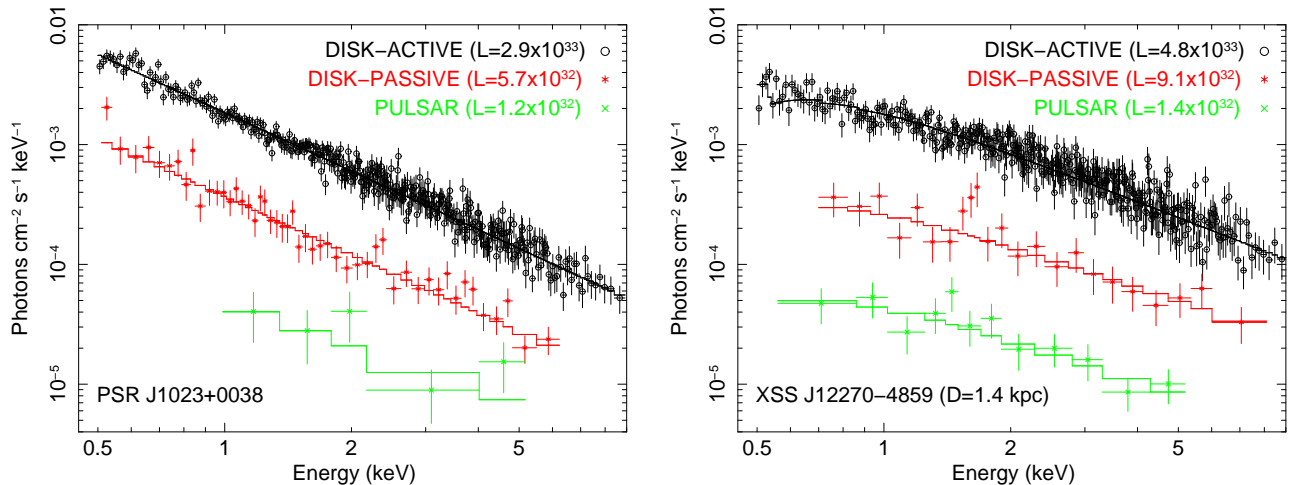


FIG. 2.— Unfolded XRT spectra of J1023 (*left*) and J12270 (*right*), together with the best fit powerlaw models, for the disk-active (black circle), disk-passive (red asterisk) and pulsar (green x) states. The 0.5–10 keV luminosity of each state is indicated, in erg s⁻¹ (see text for details). The faintest spectra are binned for display purpose only (Sec. 2, Table 1).

rates.

The two brightest redbacks, J1023 and J12270, have been observed with *Swift* in both the *pulsar state* (when radio pulsations are detected, despite being eclipsed during a fraction of the orbit) and in the *disk state* (when L_X is $\sim 10\times$ higher and double-peaked broad emission lines are observed; Archibald et al. 2009; Patruno et al. 2014; de Martino et al. 2010; Bassa et al. 2014, see Table 1 for dates and full references). We treated these subsets of observations independently, accumulating spectra and light curves for the pulsar and disk states separately. Note that the *Swift* observations were taken over the course of five years under different proposals with heterogeneous sampling and observing strategy. As a result, the accumulated exposure of disk and pulsar states in J1023 and J12270 (Figure 1, Table 1) is not representative of the intrinsic duty cycle of these states. The disk state of J1023 and J12270, however, has been extensively observed by *Swift* (48 and 18 observations, respectively). Thus we stress that the double-peaked count rate his-

tograms that we find and report in Section 3.1 are not due to a sampling effect.

3. RESULTS AND DISCUSSION

The results of our global *Swift* study allow a clear distinction between three main states of redback MRPs, in order of increasing L_X : i) pulsar state; ii) disk state and iii) outburst state. These results are summarized in Table 1, which gives also references to previous work. We present in Section 3.1 our results on the only two nearby redbacks that have shown accretion episodes, J1023 and J12270, which reveal remarkably similar X-ray properties. In the remaining 6 redbacks, discussed in Sections 3.2–3.7, there are no reports of disk emission lines, complete disappearance of radio pulsations, enhanced X-ray luminosity, X-ray bursts, pulsations or any other accretion-powered phenomenon. This strongly suggests that, to date, they have always been observed in the pulsar state. Sections 4 and 5 extend our discussion of the disk and pulsar states, respectively.

TABLE 1
LUMINOSITIES AND SPECTRA OF EIGHT NEARBY REDBACK PULSARS OBSERVED WITH *Swift*-XRT.

State	N _{obs}	Dates	Exp. (ksec)	Rate (c s ⁻¹)	L _X (0.5–10 keV; erg s ⁻¹)	Γ	N _H (10 ²¹ cm ⁻²)	χ ² /dof
PSR J1023+0038^b								
Disk-Active	43*	2013 Oct–2014 Mar	64.9	2.2×10 ⁻¹	[2.85±0.04]×10 ³³	1.62±0.02	<0.09	376.4/378
Disk-Passive	43*	2013 Oct–2014 Mar	18.7	4.4×10 ⁻²	[5.7±0.3]×10 ³²	1.62±0.07	≡0.015	43.6/48
Pulsar	2	2013 Jun	3.8	7.6×10 ⁻³	[1.6±0.5]×10 ³²	0.9±0.4	≡0.015	25.9/27 ^{CS}
XSS J12270-4859^c								
Disk-Active	18*	2005-2012	26.0	3.0×10 ⁻¹	[4.8–32]×10 ³³	1.36±0.03	0.8±0.1	395.5/393
Disk-Passive	18*	2005-2012	4.8	5.0×10 ⁻²	[9.1–60]×10 ³²	1.15±0.12	≡0.8	17.6/21
Pulsar	12	2013-2014	17.5	7.5×10 ⁻³	[1.5–9.8]×10 ³²	1.2±0.2	≡0.8	6.6/10
PSR J1628-32^d								
Pulsar	8	2013 Apr-Jun	3.2	<1.7×10 ⁻³	<2.2×10 ³¹	–	≡1.5	–
PSR J1723-28^e								
Pulsar	2	2010 Mar	6.6	2.0×10 ⁻²	[2.4±0.6]×10 ³²	0.9±0.2	≡3.4	10.0/10
PSR J1816+4510^f								
Pulsar	4	2010 Aug	4.7	<8.2×10 ⁻⁴	<1.3×10 ³²	–	≡0.3	–
PSR J2129-0429 A^g								
Pulsar	1	2010 Dec	10.4	6.0×10 ⁻³	[4.2±0.6]×10 ³¹	1.8±0.2	≡0.3	37.9/54 ^{CS}
PSR J2129-0429 B^h								
Pulsar	1	2010 Dec	10.4	2.8×10 ⁻³	[2.6±0.8]×10 ³¹	1.0±0.3	≡0.3	30.6/27 ^{CS}
PSR J2215+5135ⁱ								
Pulsar	2	2010 Jul, 2013 Dec	15.9	1.5×10 ⁻³	[1.3±0.4]×10 ³²	1.8±0.4	≡2.1	27.3/22 ^{CS}
PSR J2339-0533^j								
Pulsar	15	2009-2012	37.4	3.0×10 ⁻³	[2.7±0.5]×10 ³¹	1.4±0.3	<1.2	7.5/6
cf. IGR J18245-2452 (M28-I)^j								
Disk-Active		2008, 2013			[3.9±0.1]×10 ³³	1.51±0.04	2.9±0.2	33.3/27
Disk-Passive		2008			[5.6±1.0]×10 ³²	1.45±0.15	2.6±0.8	29.7/29
Pulsar		2002			[2.2±0.4]×10 ³²	1.2±0.2	≡2.6	294.2/647 ^{CS}

^aN_{obs}: number of *Swift* observations available in March 2014, analyzed in this work (*same set of observations where J1023 and J12270 switch between disk-active and disk-passive states). Exp.: Accumulated *Swift*-XRT (PC mode) exposure for each source/state. Rate: Net 0.5–10 keV XRT (PC mode) count rate. L_X: 0.5–10 keV luminosity using the distances given below (D). Γ: Power law index (photon flux ∝ E^{-Γ}). N_H: absorbing column density, fixed at the literature values given below when unconstrained (≡). OX: other references to previous X-ray studies. Errors (±) and upper limits (<) are given at the 68% and 90% c.l., respectively. Spectra with low number of counts (<50) were fitted using *Xspec*'s C-statistic (marked ^{CS} in the Table).

^b(D=1.37 kpc, Deller et al. 2012; N_H<1.5×10²¹ cm⁻², Bogdanov et al. 2011a; OX: Patruno et al. 2014, Archibald et al. 2010, Stappers et al. 2014, Takata et al. 2014)

^c(D=1.4–3.6 kpc, de Martino et al. 2013a; N_H=6.1×10²⁰ cm⁻², Bogdanov et al. 2014b; OX: de Martino et al. 2010, Bassa et al. 2014)

^d(D=1.2 kpc, Ray et al. 2012; N_H=1.5×10²¹ cm⁻², Kalberla et al. 2005)

^e(D=0.75 kpc, Crawford et al. 2013; N_H=3.4×10²¹ cm⁻², Bogdanov et al. 2014a; OX: Hui et al. 2014)

^f(D=4.5 kpc, Kaplan et al. 2013; N_H=0.3×10²¹ cm⁻², Kalberla et al. 2005; OX: Kaplan et al. 2012)

^g(D=0.9 kpc, Ray et al. 2012; N_H=0.3×10²¹ cm⁻², Kalberla et al. 2005. Both X-ray counterpart candidates shown, see Sec. 3.5)

^h(D=3 kpc, Ray et al. 2012; N_H=2.1×10²¹ cm⁻², Gentile et al. 2014)

ⁱ(D=1.1 kpc, N_H<1.6×10²¹ cm⁻², Romani & Shaw 2011; OX: Kong et al. 2012)

^jFor comparison, we list here the luminosity and spectral parameters of M28-I measured with *Chandra*, taken from Linares et al. (2014a) (D=5.5 kpc, Harris 1996, 2010 revision)

3.1. PSR J1023+0038 and XSS J12270-4859

J1023 was discovered as a 1.69-ms MRP in 2007 (Archibald et al. 2009, with P_{orb}=0.20 d), yet it had an accretion disk in 2000-2001 (Wang et al. 2009). J12270 was the first GeV source identified as an LMXB (de Martino et al. 2010; Hill et al. 2011; de Martino et al. 2013a) and optical observations revealed its P_{orb}=0.29 d (de Martino et al. 2013b). Their paths crossed in 2013, when J1023 reentered the disk state (Stappers et al. 2014; Patruno et al. 2014) and J12270 transitioned to a MRP phase, being observed as a rotation-powered pulsar for the first time (with also P_s=1.69 ms; Roy, Bhattacharyya & Ray 2014; Bassa et al. 2014).

Figure 1 shows the count rate histograms obtained from the light curves of the disk and pulsar states of J1023 and J12270. The distribution of count rates in the disk state of J1023 is bimodal, with two clearly dis-

tinct peaks centered around 0.04 and 0.2 c s⁻¹ (Fig. 1, left). This behavior is analogous to the mode switching observed in the disk state of M28-I (Linares et al. 2014a, see their Figure 6). The disk state of J12270 (with ~2.7 times shorter exposure) shows a similar count rate distribution (Fig. 1, right): a peak around 0.2 c s⁻¹ and a broader component at 0.01–0.1 c s⁻¹.

Using this bimodal count rate distribution, and following the nomenclature of Linares et al. (2014a), we divide the disk state into *disk-active* (>0.1 c s⁻¹) and *disk-passive* (<0.1 c s⁻¹) states. We find that during the *Swift* observations taken in the disk state, J1023 and J12270 were in the disk-active state for about 78% and 84% of the time, respectively. In contrast, M28-I was in the disk-active state for only ~60% of the 2008 *Chandra* observations (Linares et al. 2014a). Because *Swift*'s uninterrupted observing windows are short (typically ~1–2 ksec) compared to the duration of disk-active and disk-

passive states (tens of ksec), mode switching is best seen after accumulating many observations. The pulsar state observations are fainter in both sources, with average count rates 6–7 times lower than the disk-passive state.

The *Swift*-XRT spectra of the disk-active, disk-passive and pulsar states, shown in Figure 2, are all fitted satisfactorily with a simple absorbed power law model (reduced chi-squared between 0.7 and 1, Table 1). Despite the low N_H , we do not find evidence of a thermal component in the disk-active state, which has the highest signal-to-noise ratio. Using a neutron star atmosphere model (Heinke et al. 2006, with mass and radius fixed at $1.4M_\odot$ and 10km, respectively), we place upper limits on the intrinsic effective temperature of 7.3×10^5 K and 9.1×10^5 K for J1023 and J12270, respectively (a fainter thermal component has been reported by Bogdanov et al. 2011b, from *Chandra* observations of J1023). We report details of the spectral fits in Table 1, including all best-fit spectral parameters and L_X . In summary, the *Swift*-XRT spectra of J1023 and J12270 are consistent with those measured with *Chandra* in M28-I: purely non-thermal X-ray spectra with a power law photon index $\Gamma \simeq 1$ –1.5 (see Figure 2 and Table 1).

The luminosities of the disk-active, disk-passive and pulsar states of J1023 and J12270 (Table 1) are also consistent with the luminosities of the corresponding states in M28-I (Linares et al. 2014a). We therefore find conclusive evidence for *mode switching* in the disk state of J1023: a bimodal count rate distribution with non-thermal spectra and luminosity fully consistent with M28-I. This confirms the earlier suggestion based on the first *Swift* observation of the disk state of J1023 (Patruno et al. 2014). Our *Swift* results (as well as the *XMM* observations presented in de Martino et al. 2010), reveal that mode switching is also present in the disk state of J12270. Moreover, short X-ray flares are superposed on the disk-active state light curves of J12270 (see de Martino et al. 2010, for an extended discussion) and J1023 (Bogdanov, priv. comm.). These flares are most likely responsible for the high count rate tails in the histograms shown in Figure 1, as well as the small peak in the count rate distribution of the disk-active state of J12270 at ~ 0.7 c s $^{-1}$ (Fig. 1, right).

Figure 3 presents L_X and Γ for all redbacks detected with *Swift* in the pulsar and disk states. For comparison, we also show the *Chandra* results on M28-I, including the outburst state. Mode switching has now been observed in all three MRPs that have shown accretion episodes: M28-I, J1023 and J12270. Therefore, based on the currently available data, we conclude that mode switching is an ubiquitous phenomenon in the disk state of reback MRP-LMXB transition systems (see Sec. 4 for further discussion). In Figure 3 we also show the approximate boundaries between outburst and disk states ($L_X \sim 10^{34}$ erg s $^{-1}$) and between disk and pulsar states ($L_X \sim 4 \times 10^{32}$ erg s $^{-1}$), as well as a summary of the multi-wavelength properties of the three states.

It is interesting to note that the gamma-ray luminosity exceeds L_X in the pulsar, disk-passive and disk-active states (by a factor ~ 7 , ~ 10 and ~ 2 , respectively; using ~ 0.1 –300 GeV luminosities from Tam et al. 2010; Hill et al. 2011; Stappers et al. 2014). See the works by Papitto, Torres & Li (2014) and Takata et al. (2014) for

possible mechanisms to explain such gamma-ray emission, brighter in the disk state than in the pulsar state, but so far undetected in the outburst state.

If the distance to J12270 is 1.4 kpc (at the low end of the range estimated by de Martino et al. 2013a) the luminosities of the disk-active, disk-passive and pulsar states of J12270 agree with those found in M28-I and J1023 (whose distances are well known from studies of the globular cluster and from parallax measurements, respectively). This can be seen in Table 1 and Figure 3. Our results thus favor the 1.4 kpc distance estimate for J12270. For this reason we plot J12270's L_X using $D=1.4$ kpc (but we show with error bars the full L_X range allowed by the uncertainty in D). In all three systems the disk-passive state is 5–7 times fainter (lower L_X) than the disk-active state, but 3–6 times brighter (higher L_X) than the pulsar state.

3.2. PSR J1628–3205

Little is known about J1628 apart from its basic pulsar parameters ($P_{\text{orb}} \simeq 0.21$ d and $P_s \simeq 3.21$ ms, Ray et al. 2012) and its association with the *Fermi*-LAT source 2FGL J1628.3-3206 (1FGL J1627.8-3204). No X-ray or optical counterpart has been published at the time of writing, hence only the LAT (arcminute) location is available.

The eight *Swift*-XRT observations cover altogether $\sim 90\%$ of the (quasi-circular) *Fermi*-LAT error region (7.7' radius, 95% c.l.; Nolan et al. 2012). No source is detected in the summed image, and we place a 90% c.l. upper limit on the 0.5–10 keV luminosity of $L_X < 2.2 \times 10^{31}$ erg s $^{-1}$ (Table 1). This upper limit uses the total XRT exposure at the center of the LAT location (3.2 ksec). Over $\sim 40\%$ of the LAT error circle, the effective XRT exposure gradually decreases, down to ~ 0.5 ksec. If we use this exposure instead (i.e., if the X-ray counterpart is near the edge of the LAT location), the L_X upper limit becomes $\sim 10^{32}$ erg s $^{-1}$.

Figure 4 shows the upper limit on the luminosity of J1628 in the pulsar state, together with the other 7 redbacks studied in this work and M28-I. If the X-ray counterpart is near the center of the LAT location, J1628 is the reback with the lowest L_X . Deeper observations covering a slightly wider field are needed to identify the X-ray counterpart. In any case our results show that, if the LAT location is accurate, the luminosity of J1628 in the pulsar state is below 10^{32} erg s $^{-1}$.

3.3. PSR J1723–2837

J1723 is somewhat peculiar among nearby redbacks, in the sense that it was first discovered as a MRP (with $P_{\text{orb}} \simeq 0.62$ d and $P_s \simeq 1.86$ ms) with the Parkes Multibeam survey (Crawford et al. 2013, who also reported optical photometric and spectroscopic studies), and then searched and found in the X-ray and γ -ray bands (Hui et al. 2014; Bogdanov et al. 2014a).

The source is clearly detected in the two *Swift*-XRT observations, at an average $L_X = [2.4 \pm 0.6] \times 10^{32}$ erg s $^{-1}$ and $\Gamma = 0.9 \pm 0.2$. Our *Swift* results are consistent with the average L_X and Γ values measured with *Chandra* and *XMM* by Bogdanov et al. (2014a, who also find orbital modulation in L_X).

As can be seen in Figure 4 (right panel), the X-ray properties of J1723 in the pulsar state (namely, L_X and

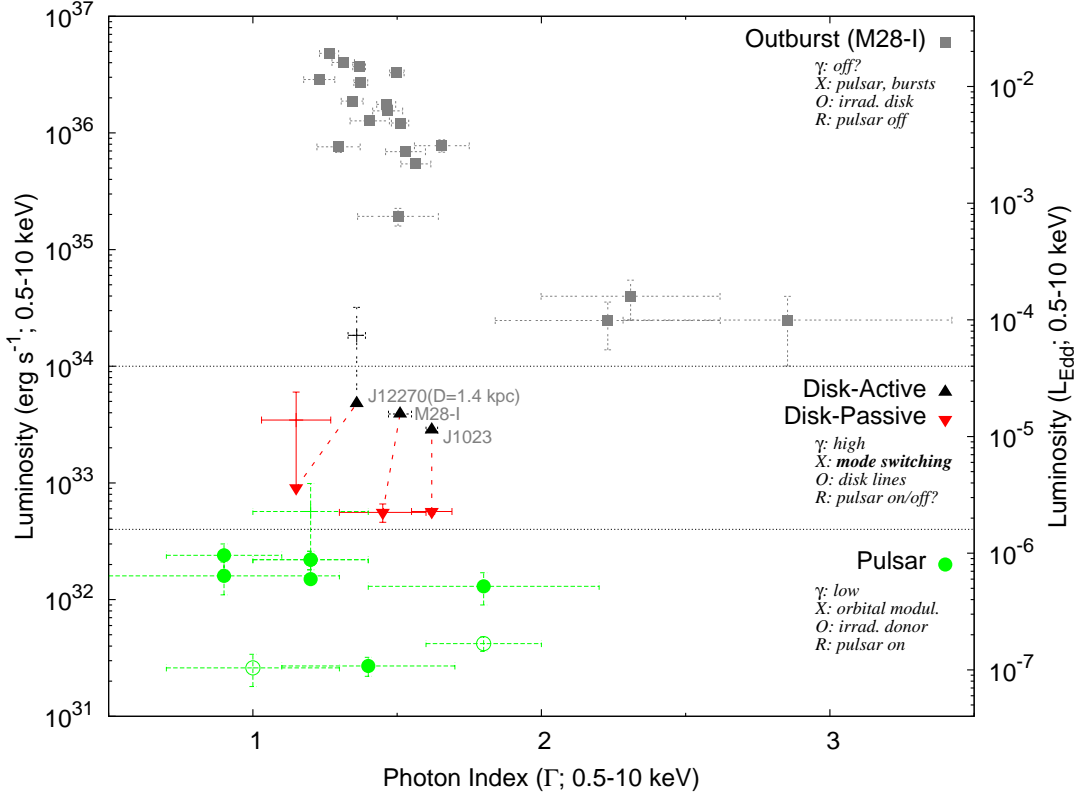


FIG. 3.— X-ray luminosity and photon index for seven redback millisecond pulsars in their three main states: pulsar (green circles; see Fig. 4 for source identification), disk (triangles) and outburst (gray squares). Approximate L_X ranges are indicated with horizontal dotted lines. Mode switching is always observed in the disk state, defining disk-active (black upward triangles) and disk-passive (red downward triangles) states, connected with red dashed lines. The main features of each state are outlined along the right axis, in the γ -ray (γ), X-ray (X), optical (O) and radio (R) bands.

Γ) are very similar to those of the three redbacks that have shown accretion: J1023, J12270 and M28-I. For this reason, we suggest that J1723 is a good candidate to develop active accretion and transition to the disk state in the near future (see Sec. 5 for further discussion).

3.4. PSR J1816+4510

J1816 was discovered by Kaplan et al. (2012) as a $P_{\text{orb}} \simeq 0.36$ d, $P_s \simeq 3.19$ ms MRP, in a Green Bank Telescope (GBT) observation targeted at the *Fermi* source 2FGL J1816.5+4511 (1FGL J1816.7+4509). The discovery and study of the optical and UV counterparts led to a sub-arcsecond location and a lower limit on the neutron star mass of $1.8 M_\odot$ (Kaplan et al. 2012, 2013).

We do not detect the source in the total 4.7 ksec *Swift*-XRT exposure, summing all four available observations, and we place an upper limit of $L_X < 1.3 \times 10^{32}$ erg s $^{-1}$ (using the revised $D=4.5$ kpc reported by Kaplan et al. 2013)⁶. Figure 4 shows our *Swift*-XRT limit on the luminosity of J1816 in the pulsar state. J1816 has a pulsar state L_X below $\sim 10^{32}$ erg s $^{-1}$, i.e., lower than the redbacks which have shown accretion episodes.

3.5. PSR J2129-0428

⁶ In a similar study of the first observation (2.8 ksec), Kaplan et al. (2012) report a 2σ c.l. flux upper limit ~ 18 times lower, which seems underestimated (their limit corresponds to a count rate of about 5×10^{-5} c s $^{-1}$ but the XRT background rate is typically $\sim 10 \times$ higher, see Sec. 2).

J2129 was also discovered as a MRP with GBT (Hessels et al. 2011; Ray et al. 2012, with $P_{\text{orb}} \simeq 0.64$ d and $P_s \simeq 7.62$ ms), in targeted observations of a LAT source (2FGL J2129.8-0428/1FGL J2129.8-0427). No X-ray counterpart has been published to date⁷. Optical studies are in progress (Bellm et al. 2013), but no accurate location has been published at the moment of writing.

The available *Swift*-XRT observation (totalling 10.4 ksec) covers the entire (quasi-circular) *Fermi*-LAT error region (8.6' radius, 95% c.l., Nolan et al. 2012). We detect two point sources inside the LAT error circle, which we name J2129A and J2129B (in order of decreasing brightness). We find the following UVOT-enhanced XRT position for J2129A: RA=21h 30m 08.16s, DEC= $-04^\circ 34' 53.8''$ (J2000; with a 90% error radius of 2.3''), which is 7.2' from the LAT position. For J2129B, the UVOT-enhanced XRT position is: RA=21h 29m 45.29s, DEC= $-04^\circ 29' 11.9''$ (J2000; with a 90% error radius of 5.8''), i.e., 1.7' from the LAT position. Given the relatively large LAT error radius (8.6'), we consider both J2129A and J2129B candidates for the X-ray counterpart of J2129 (and we plot them using open circles in Figs. 3 and 4).

⁷ Roberts et al. presented a preliminary X-ray light curve, online at http://aspen13.phys.wvu.edu/aspen_talks/Roberts_spiders.pdf, but we could not find the corresponding publication.

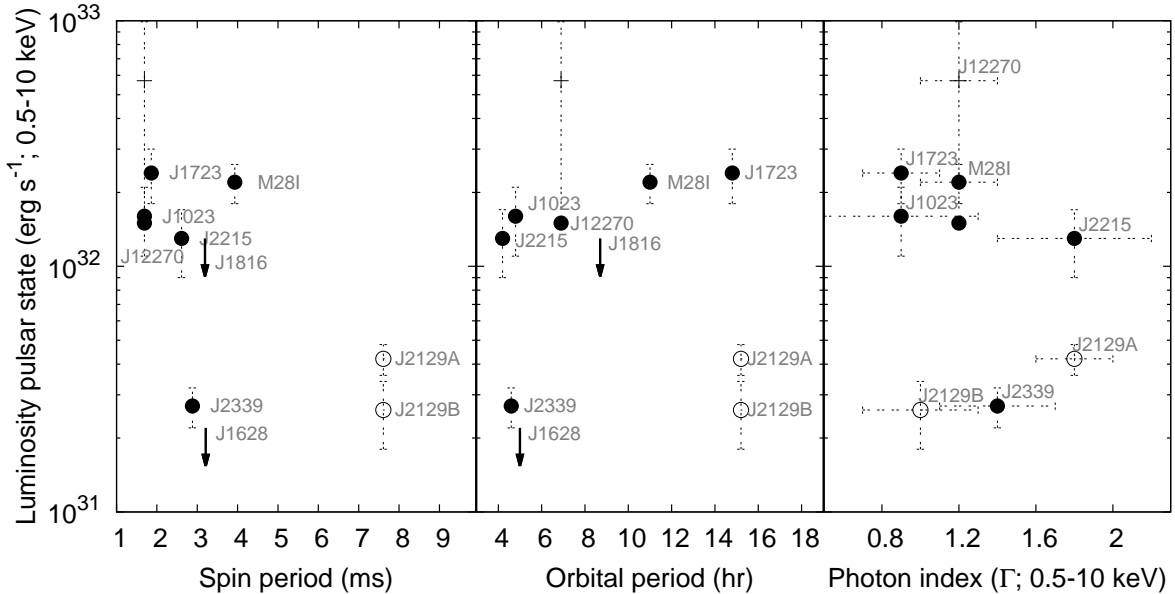


FIG. 4.— Luminosity of the pulsar state in the X-ray band (0.5–10 keV), plotted against P_s (left), P_{orb} (middle) and Γ (right). Sources are labeled and include all (eight) nearby redback MRPs studied with *Swift* in this work, as well as M28-I for comparison (Table 1). We plot the two candidate counterparts to J2129 with open circles (Sec. 3.5).

Both X-ray counterpart candidates have relatively low luminosity, $L_X \lesssim 4 \times 10^{31} \text{ erg s}^{-1}$ (see Table 1 and Figure 4). J2129A is softer ($\Gamma = 1.8 \pm 0.2$) than J2129B ($\Gamma = 1.0 \pm 0.3$). The X-ray luminosity and spectral shape of both candidates are consistent with the rest of redbacks in the pulsar state. Follow-up multi-wavelength observations are needed to identify which of our two candidates is the true counterpart to J2129. In any case, our results show that the X-ray luminosity of J2129 in the pulsar state is low, well below $10^{32} \text{ erg s}^{-1}$.

3.6. PSR J2215+5135

Discovered in radio searches of the LAT source 1FGL J2216.1+5139 (2FGL J2215.7+5135), J2215 is a 2.61 ms MRP with the shortest orbital period among Galactic field redbacks, $P_{orb} \simeq 0.17 \text{ d}$ (Hessels et al. 2011). Optical (Breton et al. 2013) and X-ray (Gentile et al. 2014) studies have identified, respectively, an irradiated companion star producing a characteristic orbital light curve and a hard, variable X-ray counterpart.

J2215 is detected in the two *Swift*-XRT observations, taken about 3.5 years apart, with no evidence of variability between the two epochs. We find $L_X = [1.3 \pm 0.4] \times 10^{32} \text{ erg s}^{-1}$ and $\Gamma = 1.8 \pm 0.4$ (Table 1; both consistent with the values reported by Gentile et al. 2014). Thus J2215 features a relatively high luminosity in the pulsar state, similar to what we find for the three MRP-LMXB transition pulsars and for J1723 (Figure 4). This suggests that J2215 is also a good candidate to show accretion episodes and transitions to the disk and outburst states in the future (Sec. 5).

3.7. PSR J2339-0533

The discovery of J2339 followed a different path: the LAT source 0FGL J2339.8-0530 was first identified as a likely MRP in a compact orbit thanks to optical photometric and spectroscopic observations, which revealed

a $P_{orb} \simeq 0.19 \text{ d}$ (Kong et al. 2011; Romani & Shaw 2011; Kong et al. 2012). More recently, radio and γ -ray pulsations have been discovered, confirming the system as a redback with $P_s \simeq 2.88 \text{ ms}$ (Ray et al. 2014).

J2339 was observed 15 times with *Swift*-XRT, in 2009, 2011 and 2012, at similar XRT count rate levels. We measure an average luminosity $L_X = [2.7 \pm 0.5] \times 10^{31} \text{ erg s}^{-1}$ and $\Gamma = 1.4 \pm 0.3$ (consistent with the values reported from a 2009 *Chandra* observation by Romani & Shaw 2011). We therefore find that J2339 is one of the four redbacks that feature low L_X in the pulsar state (well below $10^{32} \text{ erg s}^{-1}$).

4. THE DISK STATE

All three redbacks which have shown accretion episodes (J1023, J12270 and M28-I, also referred to as MRP-LMXB transition systems) have now shown mode switching in the disk state: rapid ($\lesssim 500 \text{ s}$) transitions between disk-active and disk-passive states with a factor 5–7 change in L_X and a purely non-thermal X-ray spectrum (see Table 1, Figs. 1–3 and Linares et al. 2014a). This strongly suggests that X-ray mode switching is a common phenomenon to all redbacks when they reach the accretion disk state, at $L_X \sim 10^{33} \text{ erg s}^{-1}$. Having multiple redback MRPs observed in the disk state, subtle differences begin to emerge. For instance, we find that J12270 is significantly harder than J1023 in both the disk-active and disk-passive states ($\Gamma = 1.15\text{--}1.36$ vs. 1.62). This can be seen in Figures 2 and 3.

It is worth noting that this behavior is so far unique to MRP-LMXB transition systems. To our knowledge, similar X-ray mode switching has never been observed in neutron star transients in general (transient LMXBs with no radio pulsar detected, such as Cen X-4 or 4U 1608-52; e.g., Bernardini et al. 2013) nor accreting millisecond X-ray pulsars in particular (the subset of neutron star transients showing coherent accretion-powered X-ray pulsations, such as

SAX J1808.4-3658 or Aql X-1), even though they have been observed at similar L_X (e.g., Campana et al. 1997, 1998b; Degenaar & Wijnands 2012; Coti Zelati et al. 2014). This implies a fundamental difference in the accretion flow-neutron star interaction.

As noted in Linares et al. (2014a), the two states found by Campana et al. (2008) in SAX J1808.4-3658 have different properties than the disk-active and disk-passive states of redbacks: i) they alternate on longer timescales (1–12 d), ii) they have lower luminosities ($L_X < 5 \times 10^{32}$ erg s $^{-1}$) and iii) they show a clear spectral change ($\Gamma=1.7$ –2.7). More sensitive X-ray observations have not detected rapid transitions between two clearly defined modes (e.g., Campana et al. 2002; Wijnands 2003). Furthermore, we apply the same analysis described in Sec. 2 to all available (36) *Swift*-XRT PC mode observations, extended to time bins in the 200–2000 s range, and we do not find evidence for a bimodal count rate distribution in the light curves of SAX J1808.4-3658.

The disk state of redback MRPs constitutes an intermediate stage between the (radio) pulsar state ($L_X \sim 10^{31}$ – 10^{32} erg s $^{-1}$) and a full accretion outburst ($L_X > 10^{34}$ erg s $^{-1}$, seen so far only in M28-I, Papitto et al. 2013). The non-detection of X-ray pulsations or a strong thermal component during the disk state, together with its relatively low L_X , suggests that the accretion flow in this state does not reach the neutron star surface. However, optical spectroscopy during the disk state reveals conclusive evidence of an optically thick accretion disk: broad double-peaked emission lines (Wang et al. 2009; de Martino et al. 2013b; Linares et al. 2014b). The disk states of redbacks last long (at least 6 yr and 1 yr in J12270 and J1023, respectively), and therefore a stable disk solution must exist at $L_X \sim 10^{33}$ erg s $^{-1}$.

It is interesting to study where and how this accretion disk is truncated, and for that direct observational constraints on the inner disk radius (R_{in}) are highly desirable. A rough estimate of R_{in} can be obtained from the magnetospheric radius, $R_M = 7.8 [B/10^8 \text{ G}]^{4/7} [L_{bol}/L_{Edd}]^{-2/7}$ km (the radius where magnetic and ram pressures balance; e.g., Lamb, Pethick & Pines 1973; Psaltis & Chakrabarty 1999; Patruno et al. 2009, we use here an Eddington luminosity of $L_{Edd} \equiv 2.5 \times 10^{38}$ erg s $^{-1}$). This implicitly assumes that the disk is truncated by the magnetic field of the neutron star, and a linear relation between bolometric luminosity L_{bol} and mass accretion rate in the disk (\dot{M}).

Figure 5 shows the values of R_M inferred for M28-I, J1023 and J12270 in their disk-active/passive states, compared to the corresponding corotation (R_{CO}) and light cylinder (R_{LC}) radii. We correct L_X with a bolometric factor 3 following Linares et al. (2014a) and use a value of $B=10^8$ G for the neutron star magnetic field (in accordance with the available measurements; see, e.g., Archibald et al. 2013, for J1023).

In the “tug-of-war” scenario proposed by Linares et al. (2014a) for M28-I, R_M during the disk-active state lies just inside the light cylinder (i.e., $R_M \lesssim R_{LC}$), and accretion proceeds down to the neutron star magnetosphere

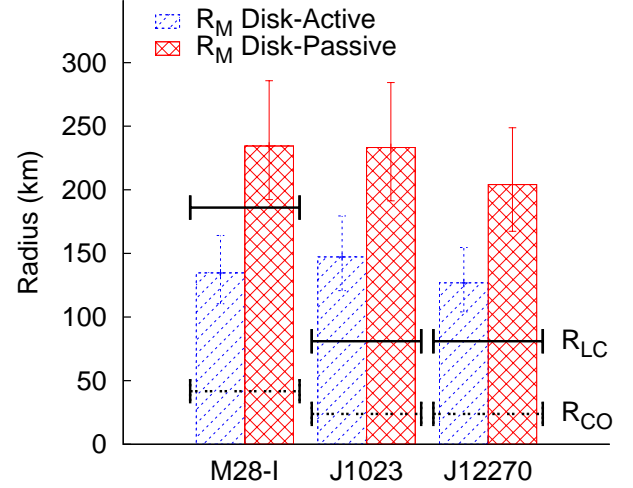


FIG. 5.— Inferred magnetospheric radius (R_M) for the disk-active (blue dashed histograms) and disk-passive (red crossed histograms) states of the three redbacks which have shown accretion (as labeled; see Sec. 4 for R_M definition). Horizontal solid and dashed black lines show the light cylinder radius (R_{LC}) and the corotation radius (R_{CO}), respectively. Error bars show the effect on R_M of increasing/decreasing the mass accretion rate by a factor 2.

(Campana et al. 1998a). Fluctuations in \dot{M} move R_M outside R_{LC} , which allows the radio pulsar to turn on. This triggers a transition to the disk-passive state, where the lower L_X is produced by a shock between the pulsar wind and the innermost accretion flow. A slight increase in \dot{M} would then push the inner edge of the disk back inside the light cylinder and turn off the radio pulsar mechanism. Thus in this simple qualitative model, supported by the inferred R_M in M28-I (Fig. 5), the X-ray mode switches reflect a dynamic balance between the accretion flow and the pulsar wind.

Let us now review this tug-of-war scenario in light of our new results on the disk state of J1023 and J12270. The light cylinder in J1023 and J12270 is a factor 2.3 smaller, due to their 2.3 times shorter P_s . Given the weak scaling of R_M with \dot{M} ($R_M \propto \dot{M}^{-2/7}$), L_X should increase by a factor of almost 20 to compensate for the factor 2.3 faster spin and bring R_M back inside the light cylinder. However, the L_X of J1023, J12270 (for $D=1.4$ kpc) and M28-I in the active/passive states are consistent within a factor <1.7 (Table 1). Therefore, we find that there is no strong dependence of the disk state luminosity (and the inferred R_{in}) on the pulsar’s spin or orbital period (P_{orb} in J1023 is also about 2.3 times shorter than M28-I). This argues against the tug-of-war model in its simplest form: as shown in Figure 5, R_M does not cross the light cylinder in the case of J1023 and J12270 when going from the disk-active to the disk-passive state.

The R_M shown in Figure 5 suggest that J1023 and J12270 (with $R_M > R_{LC}$) may also harbor a rotation-powered pulsar in the disk state (both active and passive). However, we stress that a more detailed physical model of the transition between accretion and rotation power is needed to confirm this, one that goes beyond the magnetospheric radius prescription. Extensive radio observations of the disk-passive state can help understand

its nature, assessing whether or not the rotation-powered pulsar is on.

Forces other than magnetic, such as radiation pressure from the radio pulsar, are expected to act upon the inner accretion disk. Ekşİ & Alpar (2005) studied the truncation and stability of accretion disks around radio pulsars. They found that the radiation pressure of a rotation-powered pulsar does not necessarily disrupt a surrounding disk, and therefore an accretion disk and an active MRP can coexist. According to their model, stable disk solutions exist with $R_{\text{in}} > R_{\text{LC}}$, up to more than ten times R_{LC} if the neutron star's magnetic inclination (angle between spin and magnetic axes) is small (Ekşİ & Alpar 2005). In this context, we note that our highest estimate of the magnetospheric radius in the disk-active state, $R_{\text{M}} \simeq 147 \text{ km} \simeq 1.8 \times R_{\text{LC}}$ in J1023, only has stable solutions for magnetic inclinations lower than 15° (Ekşİ & Alpar 2005). This might indicate that redbacks have nearly aligned rotating dipoles, although more detailed models tailored to the disk state of redback MRPs are required to make quantitative statements. In any case, our results strongly support the presence of a stable accretion disk around redback millisecond pulsars with $R_{\text{in}} > R_{\text{LC}}$. Hence this new class of pulsars holds great potential to study accretion flows near the light cylinder.

We measure an X-ray flux of 0.6 mCrab in the brightest disk-active state in our sample (J12270), i.e., more than ten times fainter than the 1-day sensitivity limits of currently active all-sky X-ray monitors (*MAXI*: 8 mCrab at 5σ , Matsuoka et al. 2009; *Swift*-BAT: 16 mCrab at 3σ , Krimm et al. 2013). Longer exposures (Hiroi et al. 2013; Krimm et al. 2013) or improved all-sky monitors, such as the Wide-Field Monitor onboard the proposed *LOFT* mission⁸, may be able to detect new transitions of redbacks to the disk state. Until then, *Swift*-XRT monitoring provides the most efficient way of catching state transitions in nearby redback millisecond pulsars.

An interesting question for future study is when exactly (at which L_{X}) accretion-powered X-ray pulsations appear, and whether or not this coincides with the complete disappearance of rotation-powered radio pulsations. Papitto et al. (2013) set an upper limit of 17% on the pulsed fraction of M28-I at $L_{\text{X}} \sim 10^{33} \text{ erg s}^{-1}$. The redbacks compiled in this work offer the best prospects in this respect, and given their short D and low N_{H} they should allow a much more sensitive search for X-ray pulsations at low L_{X} . For instance, the collected X-ray count rates in the disk-active state of J12270 (4.8 and 6.4 c s^{-1} with *XMM* and the approved *NICER* mission, respectively⁹) are 25 times higher than those for M28-I at the same L_{X} .

5. THE PULSAR STATE

By studying the full sample of redbacks selected for this work, we find that the X-ray luminosity of the pulsar state is in the 10^{31} – $10^{32} \text{ erg s}^{-1}$ range, always lower than that of the disk state (Fig. 3). Moreover, redbacks can be roughly divided in two groups based on their luminosity in the pulsar state (Figure 4): those having relatively high L_{X} ($\gtrsim 10^{32} \text{ erg s}^{-1}$: M28-I, J1023, J12270, J1723

and J2215) and those having low L_{X} ($< 10^{32} \text{ erg s}^{-1}$: J1628, J2339, J2129 and probably J1816). The XRT spectra of the pulsar state are hard, with Γ between 0.9 and 1.8. We do not find strong dependence of L_{X} or Γ on P_{s} , P_{orb} or M_{C} .

Based on their high pulsar state luminosities, we suggest that J1723 and J2215 are good candidates to show accretion episodes in the near future (Secs. 3.3 and 3.6). A higher L_{X} may indicate stronger interaction with the companion star, due to a higher spin-down luminosity or to a larger fraction of the pulsar wind being shocked. More intense ablation of the companion's heated face could result into enhanced mass transfer, and potentially feed accretion disk episodes such as those seen in J1023 and J12270. More sensitive X-ray missions are better suited to study in detail this state (Bogdanov et al. 2011a, 2014b), although we have shown that *Swift*-XRT can detect nearby redbacks in the pulsar state with moderate exposure times ($\sim 10 \text{ ksec}$), down to just a few times $10^{31} \text{ erg s}^{-1}$. Measurements of the radio pulsar spin-down rate may be possible soon for more redbacks, and together with the luminosities reported herein will help constrain the energetics of the pulsar wind shock.

6. SUMMARY AND CONCLUSIONS

Redbacks have provided the long-sought link between MRPs and LMXBs, and we are in the process of understanding their properties as a class. They allow us to study in an unprecedented way the transition between accretion and rotation power around neutron stars, as well as the interaction between millisecond pulsars and accretion flows.

We have presented the first systematic X-ray study of redback millisecond pulsars, using more than 100 *Swift* observations of eight nearby systems and covering luminosities between 10^{31} and $10^{34} \text{ erg s}^{-1}$. We next summarize our main results and conclusions.

- The X-ray luminosity of redbacks can vary by six orders of magnitude, defining three main states: i) *outburst state* ($10^{34} < L_{\text{X}} < 10^{37} \text{ erg s}^{-1}$), seen only in one system to date; ii) *disk state* ($4 \times 10^{32} < L_{\text{X}} < 10^{34} \text{ erg s}^{-1}$), observed in three systems to date; and iii) *pulsar state* ($10^{31} < L_{\text{X}} < 4 \times 10^{32} \text{ erg s}^{-1}$), where at least seven redbacks have been detected in X-rays.
- All redbacks which have transitioned to the disk state (J1023, J12270 and M28-I) have shown *X-ray mode switching*: fast back-and-forth transitions between disk-active and disk-passive states, with a factor 5–7 change in luminosity. This strongly suggests that mode switching, which has not been observed in “normal” LMXBs, is a universal phenomenon of redbacks in the disk state.
- The current sample of redbacks can be roughly divided in two groups according to their luminosity in the pulsar state (bright or faint, above or below $10^{32} \text{ erg s}^{-1}$). All three redbacks which have shown evidence for accretion (J1023, J12270 and M28-I), have $L_{\text{X}} > 10^{32} \text{ erg s}^{-1}$. Based on this we suggest that J1723 and J2215 are promising candidates to develop accretion disks.

⁸ <http://sci.esa.int/loft/53447-loft-yellow-book/>

⁹ <http://heasarc.gsfc.nasa.gov/Tools/w3pimms.html>

Acknowledgments:

I am most grateful to A. Alpar and J. Homan for their insightful comments on the manuscript, to M. Roberts for a conversation that sparked this work and to S. Bogdanov for sharing his XMM results on J1023. I also

thank the anonymous referee for constructive comments that improved the paper. This research has made use of data obtained from NASA's High Energy Astrophysics Science Archive Research Center (HEASARC), and data supplied by the UK Swift Science Data Center at the University of Leicester.

REFERENCES

- Abdo A. A. et al., 2010, *ApJS*, 188, 405
- Alpar M. A., Cheng A. F., Ruderman M. A., Shaham J., 1982, *Nature*, 300, 728
- Archibald A. M., Kaspi V. M., Bogdanov S., Hessels J. W. T., Stairs I. H., Ransom S. M., McLaughlin M. A., 2010, *ApJ*, 722, 88
- Archibald A. M., Kaspi V. M., Hessels J. W. T., Stappers B., Janssen G., Lyne A., 2013, Submitted to *ApJ*; *ArXiv* 1311.5161
- Archibald A. M. et al., 2009, *Science*, 324, 1411
- Arnaud K. A., 1996, in *Astronomical Society of the Pacific Conference Series*, Vol. 101, *Astronomical Data Analysis Software and Systems V*, Jacoby G. H., Barnes J., eds., pp. 17–+
- Arons J., Tavani M., 1993, *ApJ*, 403, 249
- Bassa C. G. et al., 2014, *MNRAS*, 441, 1825
- Begin S., 2006, Master's thesis, Faculty of Physics, UBC
- Bellm E. et al., 2013, in *American Astronomical Society Meeting Abstracts*, Vol. 221, *American Astronomical Society Meeting Abstracts*, p. 154.10
- Bernardini F., Cackett E. M., Brown E. F., D'Angelo C., Degenaar N., Miller J. M., Reynolds M., Wijnands R., 2013, *MNRAS*, 436, 2465
- Bogdanov S., Archibald A. M., Hessels J. W. T., Kaspi V. M., Lorimer D., McLaughlin M. A., Ransom S. M., Stairs I. H., 2011a, *ApJ*, 742, 97
- Bogdanov S., Esposito P., Crawford, III F., Possenti A., McLaughlin M. A., Freire P., 2014a, *ApJ*, 781, 6
- Bogdanov S., Grindlay J. E., van den Berg M., 2005, *ApJ*, 630, 1029
- Bogdanov S., Patruno A., Archibald A. M., Bassa C., Hessels J. W. T., Janssen G. H., Stappers B. W., 2014b, Submitted to *ApJ*; *ArXiv* 1402.6324
- Bogdanov S. et al., 2011b, *ApJ*, 730, 81
- Breton R. P. et al., 2013, *ApJ*, 769, 108
- Brown E. F., Bildsten L., Rutledge R. E., 1998, *ApJL*, 504, L95
- Camilo F., Lorimer D. R., Freire P., Lyne A. G., Manchester R. N., 2000, *ApJ*, 535, 975
- Campana S., Colpi M., Mereghetti S., Stella L., Tavani M., 1998a, *A&ARv*, 8, 279
- Campana S., Mereghetti S., Stella L., Colpi M., 1997, *A&A*, 324, 941
- Campana S. et al., 2008, *ApJL*, 683, L9
- Campana S. et al., 2002, *ApJL*, 575, L15
- Campana S., Stella L., Mereghetti S., Colpi M., Tavani M., Ricci D., Fiume D. D., Belloni T., 1998b, *ApJL*, 499, L65+
- Coti Zelati F., Campana S., D'Avanzo P., Melandri A., 2014, *MNRAS*, 438, 2634
- Crawford F. et al., 2013, *ApJ*, 776, 20
- D'Amico N., Possenti A., Manchester R. N., Sarkissian J., Lyne A. G., Camilo F., 2001, *ApJL*, 561, L89
- de Martino D. et al., 2013a, *A&A*, 550, A89
- de Martino D. et al., 2013b, *The Astronomer's Telegram*, 5651, 1
- de Martino D. et al., 2010, *A&A*, 515, A25
- Degenaar N., Wijnands R., 2012, *MNRAS*, 422, 581
- Deller A. T. et al., 2012, *ApJL*, 756, L25
- Eksi K. Y., Alpar M. A., 2005, *ApJ*, 620, 390
- Evans P. A. et al., 2009, *MNRAS*, 397, 1177
- Ferrigno C. et al., 2014, *A&A*, 567, A77
- Fruchter A. S., Stinebring D. R., Taylor J. H., 1988, *Nature*, 333, 237
- Gentile P. A. et al., 2014, *ApJ*, 783, 69
- Goad M. R. et al., 2007, *A&A*, 476, 1401
- Harris W. E., 1996, *AJ*, 112, 1487
- Heinke C. O., Rybicki G. B., Narayan R., Grindlay J. E., 2006, *ApJ*, 644, 1090
- Hessels J. W. T. et al., 2011, in *American Institute of Physics Conference Series*, Vol. 1357, *American Institute of Physics Conference Series*, Burgay M., D'Amico N., Esposito P., Pellizzoni A., Possenti A., eds., pp. 40–43
- Hill A. B. et al., 2011, *MNRAS*, 415, 235
- Hiroi K. et al., 2013, *ApJS*, 207, 36
- Hui C. Y., Tam P. H. T., Takata J., Kong A. K. H., Cheng K. S., Wu J. H. K., Lin L. C. C., Wu E. M. H., 2014, *ApJL*, 781, L21
- Kalberla P. M. W., Burton W. B., Hartmann D., Arnal E. M., Bajaja E., Morras R., Pöppel W. G. L., 2005, *A&A*, 440, 775
- Kaplan D. L., Bhallerao V. B., van Kerkwijk M. H., Koester D., Kulkarni S. R., Stovall K., 2013, *ApJ*, 765, 158
- Kaplan D. L. et al., 2012, *ApJ*, 753, 174
- Kong A. K. H. et al., 2012, *ApJL*, 747, L3
- Kong A. K. H., Huang R. H. H., Tam P. H. T., Cheng K. S., Takata J., Hui C. Y., 2011, in *American Astronomical Society Meeting Abstracts #218*, p. 320.05
- Krimm H. A. et al., 2013, *ApJS*, 209, 14
- Lamb F. K., Pethick C. J., Pines D., 1973, *ApJ*, 184, 271
- Linares M. et al., 2014a, *MNRAS*, 438, 251
- Linares M., Casares J., Rodriguez-Gil P., Shahbaz T., 2014b, *The Astronomer's Telegram*, 5868, 1
- Matsuoka M. et al., 2009, *PASJ*, 61, 999
- Nolan P. L. et al., 2012, *ApJS*, 199, 31
- Papitto A. et al., 2013, *Nature*, 501, 517
- Papitto A., Torres D. F., Li J., 2014, *MNRAS*, 438, 2105
- Patruno A. et al., 2014, *ApJL*, 781, L3
- Patruno A., Watts A., Klein Wolt M., Wijnands R., van der Klis M., 2009, *ApJ*, 707, 1296
- Possenti A., D'Amico N., Manchester R. N., Camilo F., Lyne A. G., Sarkissian J., Corongiu A., 2003, *ApJ*, 599, 475
- Psaltis D., Chakrabarty D., 1999, *ApJ*, 521, 332
- Ray P. S. et al., 2012, 2011 Fermi Symposium proceedings - eConf C110509; *ArXiv* 1205.3089
- Ray P. S. et al., 2014, in *American Astronomical Society Meeting Abstracts*, Vol. 223, *American Astronomical Society Meeting Abstracts*, p. 140.07
- Roberts M. S. E., 2011, in *American Institute of Physics Conference Series* (arXiv: 1103.0819), Vol. 1357, *American Institute of Physics Conference Series*, Burgay M., D'Amico N., Esposito P., Pellizzoni A., Possenti A., eds., pp. 127–130
- Roberts M. S. E., 2013, in *IAU Symposium* (arXiv:1210.6903), Vol. 291, *IAU Symposium*, pp. 127–132
- Romani R. W., Shaw M. S., 2011, *ApJL*, 743, L26
- Roy J., Bhattacharyya B., Ray P., 2014, *The Astronomer's Telegram*, 5890, 1
- Stappers B. W. et al., 2014, *ApJ*, 790, 39
- Stappers B. W., Gaensler B. M., Kaspi V. M., van der Klis M., Lewin W. H. G., 2003, *Science*, 299, 1372
- Takata J. et al., 2014, *ApJ*, 785, 131
- Tam P. H. T. et al., 2010, *ApJL*, 724, L207
- Tauris T. M., 2012, *Science*, 335, 561
- Tendulkar S. P. et al., 2014, *ArXiv e-prints* (astro-ph 1406.7009)
- Wang Z., Archibald A. M., Thorstensen J. R., Kaspi V. M., Lorimer D. R., Stairs I., Ransom S. M., 2009, *ApJ*, 703, 2017
- Wijnands R., 2003, *ApJ*, 588, 425
- Wijnands R., Miller J. M., Markwardt C., Lewin W. H. G., van der Klis M., 2001, *ApJL*, 560, L159

¹⁰ After this work was submitted, Tendulkar et al. (2014) published results from a *NuStar* hard X-ray study of J1023. They find two distinct states in the October 2013 observation of J1023

(which they call dip and non-dip states) with timescales, luminosity and spectral shape similar to the disk-passive and disk-active states that we report and discuss herein.